A Novel Type of Utility-Interactive Inverter for Photovoltaic System

Yasuyuki NISHIDA and Naoyuki AIKAWA

Dept. of Electrical & Electronic Engineering, Nihon Univ.
Tokusada, Tamura, Kouriyama, 963-8642 JAPAN
E-mail: nishida@ee.ce.nihon-u.ac.jp

Shinichiro SUMIYOSHI, Hidekazu YAMASHITA and Hideki OMORI

Matsushita Electric Industrial Co., Ltd
2-2-8, Nihode-machi, Toyonaka, Osaka, 561-0821 JAPAN

***Abstract*—A novel utility-interactive inverter for photovoltaic system is proposed. This inverter has no transformer to reduce the size but has a unique power processing system consisting of a dc-dc converter and a single-phase semi-bridge inverter. The dc-dc converter is a two-quadrant type and performs boost/buck-mode operations to feed-forward/feed-back the instantaneous power to/from the utility. The feed-backing function is rarely utilized for such as controlling the power-factor in utility side to regulate the utility voltage.**

***Although both the dc-dc converter and the inverter operate with high-frequency switching at all the time in the conventional scheme, only the dc-dc converter or the inverter operate with high-frequency switching in the proposed one. Thus, the switching losses are reduced significantly in the new system. Additionally, the dc-dc converter controls the input current so that the dc-inductor traps the ripple-power fed back from the utility. As a result, a large capacitor is not necessary to connect in the input of inverter in this new system.**

***In the products, the efficiency marked very high value (i.e., 95.5 [%] and 95.1 [%] in the half-load and the rated full-load condition of 4.5kW, respectively) where the utility voltage is 240 [V_{RMS}] and the solar-cells voltage is 200 [V]. On the other hand, the Total-Harmonic-Distortion of the utility current of the product marked very low value (i.e., 1.6 [%]) in the rated condition. The size of the power unit including the heat sink is reduced to 2/3 of the conventional one.**

Keywords—bidirectional dc-dc converter, photovoltaic, single-phase PWM inverter, utility interactive

I. INTRODUCTION

As the market of the utility interactive photovoltaic system has been growing the demand for improving the system efficiency and reducing the size, weight and cost have been becoming significant. The high-frequency transformer utilized system[1] is an attractive one to obtain isolation between the solar-cells side and the utility side. However, the transformer-less type is much more attractive from the viewpoint of improving the efficiency, size, weight and cost. Thus, the transformer-less type has been becoming the dominant one. In this transformer-less system, a boost-type dc-dc converter and an inverter cascade scheme is chosen usually. The boost dc-dc converter is for obtaining a stable and higher dc-input voltage of the inverter from an unstable and lower voltage fed from the solar-cells. In such single-phase system, a large capacitance capacitor is connected in the input of the inverter to trap the ripple energy fed from the utility so that the input voltage is kept constant/stable. Further, both the dc-dc converter and the inverter operate with high-frequency switching at all the time and a high amount of switching losses are produced. To overcome the problems, the authors have developed a novel and smart solution.

In the proposed utility interactive inverter system, the waveform of the input current of the dc-dc converter (i.e., the waveform of the dc-inductor current in the input) is waveshaped by bang-bang control so that the dc-inductor traps the ripple-power fed back from the utility. This control is available in the period (called "Period-A" hereafter) where the solar-cells output-voltage (V_{SOLAR}) is lower than the absolute-value of the utility voltage ($|v_{UTIL}|$). Thus, a large capacitor employed in the conventional system and connected in the dc-link-stage between the dc-dc converter and the inverter to trap the ripple power is no longer necessary in this new system. As a result, the power unit of the proposed system becomes compact. Further, since the utility current is controlled to draw a sinusoidal waveform in phase with the utility voltage by this current control of the dc-dc converter, the inverter is not necessary to control the utility current waveform. As a result, the inverter does not require switching in this period where $V_{SOLAR} < |v_{UTIL}|$. Therefore, the switching losses are reduced and the efficiency is improved. In the remaining period (called "Period-B" hereafter) where $V_{SOLAR} > |v_{UTIL}|$, the dc-dc converter cannot operate due to the boost-mode nature. Instead, the inverter performs the waveshaping of the utility current by high-frequency switching PWM with the bang-bang control.

Applying this new waveshaping scheme, the above-mentioned large capacitor employed in the conventional system can be removed and a compact system is realized. Further, only the boost dc-dc converter or the inverter operates with high-frequency switching at all the time in the proposed system and thus, the switching frequency is reduced in average and the efficiency is improved in the new system.

The power circuit topology and current control theory have been discussed below. Then, experimental results obtained from a product have been shown to confirm the validity of the theory and to demonstrate the practicability of the proposed scheme.

II. POWER CIRCUIT TOPOLOGY

Fig. 1 shows the proposed utility interactive photovoltaic system. The power circuit consists of solar-cells (the output voltage is V_{DC1}), a two-quadrant dc-dc converter, a suppressed capacitor C_2 (film capacitor), a single-phase inverter, an ac filtering inductor L_2, a noise-filter NF and a utility of single-phase 240 [V_{RMS}]. The diode D_S in the dc-dc converter is to modify the topology and it has been omitted here. The operation with the diode D_S is discussed later.

The two-quadrant dc-dc converter consists of an electrolytic capacitor C_1, a dc-inductor L_1 and two reverse-conducting switching arms. This converter feeds the power produced by the solar-cells to the utility via the inverter with the boost-mode operation by means of the switch SW_F and the reverse conducting diode D_B. While the converter performs the buck-mode operation by means of the switch SW_B and the reverse conducting diode D_F to feed the power buck from the utility to the capacitor C_1.

Comparing to the conventional system with the similer topology, the dc-capacitor C_2 on the input-side of the inverter is suppressed significantly as introduced below.

III. UTILITY CURRENT CONTROL

The control of the utility current i_S in the proposed system is unique and it's achieved by means of both the dc-dc converter and the inverter.

A. Operation and Current Control of DC-DC Converter

This dc-dc converter is a two-quadrant type, and it feeds the power obtained from the solar-cells to the inverter with boost-mode operation. On the other hand, it feeds the energy back from the utility to the dc capacitor C_1 with buck-mode operation. The energy feedback with the buck-mode operation is rarely utilized to control the power factor of the utility to reduce the utility voltage. Since this case is occurred very rarely and is not focus here, the detail is omitted in this paper.

Since the voltage produced by the solar-cells is not high enough to obtain certain level of ac-voltage through the inverter, a boost-mode dc-dc converter is necessary to connect between the solar-cells and the inverter in the transformer-less system. In this project, however, the solar-cells unit is designed to produce the output voltage of approximately 200 [V] in the maximum output power condition (i.e., 4.5kW).

A higher voltage can be obtained depending on solar-cells arrangement but it affects reasonable system designing. On the other hand, the inverter needs approximately 400 [V] or more in the conventional system since the utility voltage is up to 280 [V_{RMS}] and the maximum value reaches almost 400 [V].

When the solar-cells voltage V_{DC1} is greater than the absolute value of the utility voltage $|v_{AC}|$, the inverter operates only as a polarity switcher, i.e., it connects the positive/negative dc-rail to the higher/lower potential rail on the ac-side. This period is called "Period-A" hereafter. Since the inverter does not perform any switching in this period, the absolute value of the ac-voltage $|v_{AC}|$ appears on the dc-side (i.e., $v_{DC2} = |v_{AC}|$). However, the inductance of the ac-inductor L_2 is very low (its %-reactance in the products is only 2.5%) and the voltage drop is negligible. Thus, the inverter dc-input voltage v_{DC2} equals the absolute value of the utility voltage $|v_S|$ (i.e., $v_{DC2} = |v_S|$).

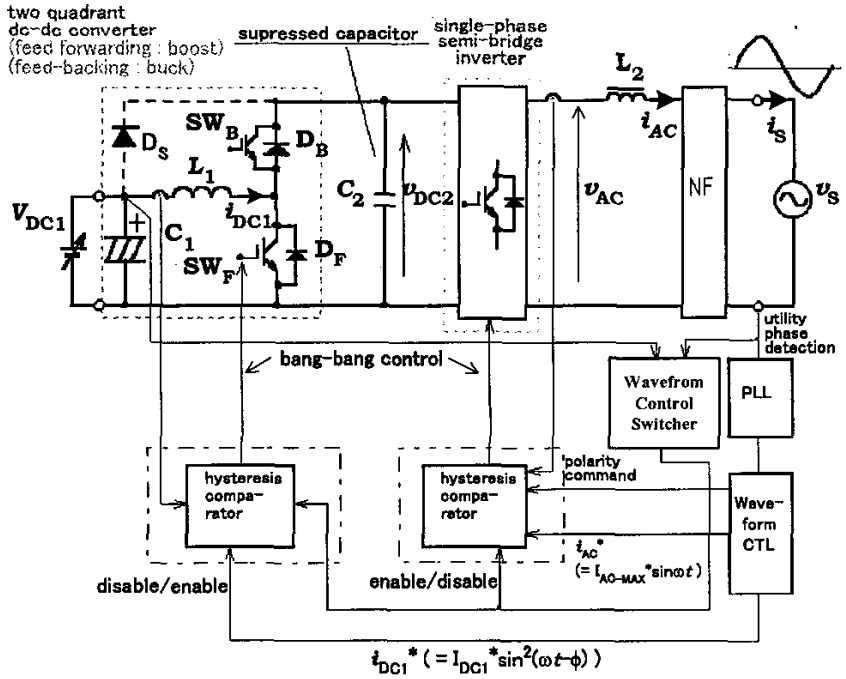

Fig. 1. Proposed Utility Interactive Photovoltaic System.

As a result, the solar-cells voltage (i.e., dc-dc converter input voltage) V_{DC1} is lower than the output voltage v_{DC2}. Therefore, the dc-dc converter can perform a boost-mode operation in this period.

If the PFC is achieved somehow, the utility current i_S draws a sinusoidal waveform in-phase with the utility voltage v_S. Thus, the instantaneous power p_S fed from the utility is expressed as;

$$p_S = 2V_{S\text{-}RMS} I_{S\text{-}RMS} \sin^2 \omega t, \quad \ldots(1)$$

where $V_{S\text{-}RMS}$ and $I_{S\text{-}RMS}$ are the RMS-values of the utility voltage and current, respectively.

Since the series and parallel impedance of the noise-filter NF is enough low and high, respectively, its series voltage drop and parallel by-pass current are negligible. Further, if drop-voltages, bypass-currents and losses of the inverter, capacitor C_2 and the dc-inductor L_1 are all neglected, the instantaneous power p_S fed to the utility equals the instantaneous dc-power p_{DC1} ($=V_{DC1} i_{DC1}$). Thus, we obtain;

$$p_S = p_{DC1} = V_{DC1} i_{DC1}. \quad \ldots(2)$$

From equations (1) and (2), we obtain;

$$\begin{aligned} i_{DC1} &= p_S / V_{DC1} \\ &= \left(2V_{S\text{-}RMS} I_{S\text{-}RMS} \sin^2 \omega t\right) / V_{DC1} \quad \ldots(3) \\ &= I_{DC1} \sin^2 \omega t, \end{aligned}$$

where

$$I_{DC1} = 2V_{S\text{-}RMS} I_{S\text{-}RMS} / V_{DC1}. \quad \ldots(4)$$

However, if we can force the dc-current i_{DC1} to produce the waveform shown in Eq. (4), the PFC is achieved. The dc-current i_{DC1} is the input current of the boost dc-dc converter, and its waveform is controllable when the input voltage V_{DC1} is lower than the output voltage v_{DC2}, i.e., in the discussing condition in Period-A. To realize the waveform control, the following current reference i_{DC1}* is generated in the part "Waveform CTL" shown in Fig. 1.

$$i_{DC1}^* = I_{DC1}^* \sin^2(\omega t + \phi), \quad \ldots(5)$$

where

$$I_{DC1}^* = 2V_{S\text{-}RMS} I_{S\text{-}RMS}^* / V_{DC1}. \quad \ldots(6)$$

The RMS-value and average-value of voltages (i.e., $V_{S\text{-}RMS}$ and V_{DC1}) on the right-hand-side in Eq. (6) are detected through sensors in the system. It notes that the capacitor voltage V_{DC1} can be regarded as constant since capacitance of C_1 is large enough. $I_{S\text{-}RMS}$* on the right-hand-side in Eq. (6) is the reference of the RSM-value of the utility current i_S, and it determines the power fed from the solar-cells to the utility. Thus, this value is determined in the "Maximum Power Tracking" control part (not shown in Fig. 1) in the control system and fed to "Waveform CTL" shown in Fig. 1. The "Maximum Power Tracking" control in the system is based on a conventional one and its detail is omitted in this paper.

In practice, however, the capacitor C_2 produces a phase displacement between the dc-inductor current i_{DC1} and the utility current i_S, and it results in decrease of the power-factor. To take the displacement into account in the control, a displacement phase-angle ϕ is set in the reference i_{DC1}* as shown in Eq. (5). The phase-angle ϕ is adjusted in the "Waveform CTL" by referring to the detected displacement phase-angle between the utility voltage v_S and current i_S. This is the principle how to control the instantaneous input current i_{DC1} of the dc-dc converter to achieve the PFC in Period-A. The actual current i_{DC1} is controlled to follow the reference with so called Bang-Bang control by means of a "histeresis controller." This PFC theory is based on the instantaneous control for the energy stored in the dc-inductor L_1 and is applicable to difference topologies[2].

B. Operation and Current Control of Inverter

As shown in Fig. 2, the inverter consists of two half-bridges; the half-bridge on the left-hand-side is with two high-frequency type switches ($SW_{HF\text{-}P}$ and $SW_{HF\text{-}N}$) while the other half-bridge on the right-hand-side is with two low-frequency switches ($SW_{LF\text{-}P}$ and $SW_{LF\text{-}N}$). As mentioned, this inverter (i.e., all the four switches) operates without switching in the Period-A so that the positive/negative dc-rail is connected to the higher/lower potential ac-rail at all the time in the Period-A. In this period, the boost dc-dc converter plays the role to achieve the PFC. On the other hand, the inverter plays the role in the remaining period (called "Period-B" hereafter), and the high-frequency switches (i.e., $SW_{HF\text{-}P}$ and $SW_{HF\text{-}L}$) operate alternately each other with a high-frequency. This switching is controlled based on the Bang-Bang control by means of the "histeresis controller" as shown in Fig. 3. The waveform (i.e., "sinωt") of the reference i_{AC}* is generated in "Waveform CTL" referring to the detected utility voltage v_S while the amplitude $I_{AC\text{-}MAX}$* is determined based on "Maximum Power Tracking" control. By means of the information (i.e., "sinωt" and $I_{AC\text{-}MAX}$*) the reference i_{AC}* is synthesized in the "Waveform CTL."

Since the dc-voltage v_{DC2} is greater than the absolute value $|v_{AC}|$ of the ac-voltage v_{AC} in this Period-B, the inverter can control the ac-current i_{AC} to follow the reference i_{AC}*.

C. Summing up the operation and comparing to conventional scheme

As discussed in Section A and B, only one of the two power converters (i.e., the boost dc-dc converter in Period-A or the inverter in Period-B) operates in high-frequency switching and other one interrupts the switching in this proposed scheme as shown in **Fig. 3**. On the other hand, both the power converters operate with high-frequency switching at all the time in conventional schemes. Thus, the switching losses are significantly reduced in the proposed one. Additionally, a part of conduction losses produced in the inverter is reduced since switches with lower forward-voltage-drop are applicable for the low-frequency half-bridge. As a result, the losses

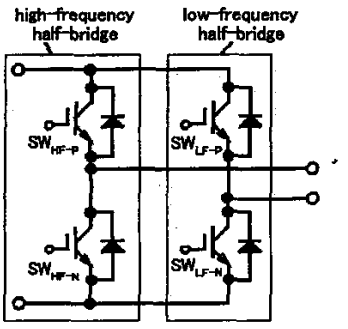

Fig. 2. Inverter.
It consists of a high-frequency half-bridge with fast IGBTs and a low-frequency half-bridge with slower IGBTs.

and the size of the power unit (including the two power converters and a heat-sink) decrease. Further, the bulky electrolytic capacitor with a large capacitance connected in the input of the inverter in the conventional products is replaced by a small film capacitor C_2 in the new products. Due to the new topology and control, the proposed system becomes advantageous for the conventional one in size, weight, cost and maintenance.

However, it is difficult to compress both the capacitor C_1 and C_2 at the same time but C_1 can be compressed instead of C_2. In this case, the total size and cost of the two capacitors is almost the same to the proposed one but the inverter input voltage v_{DC2} becomes smooth. Thus, the boost dc-dc converter cannot control the ac current i_{AC} or the utility current i_S. As a result, both the dc-dc converter and the inverter must operate PWM at all the time. Therefore, the switching loss reduction and the utilization of cheep and low forward-voltage-drop switches are no longer applicable in this case. From the practical view of point, the proposed topology and control scheme is reasonable to realize a utility interactive inverter system with cheap, low losses, light weight and compact size.

This inverter is, however, designed as a home appliance, and acoustic noise must be low. Thus, the air-forced-cooling is difficult to apply. In such the condition, low loss property is essential and the proposed loss reducing technique is desirable.

IV. PRODUCTS AND PRACTICAL EVALUATION

To confirm the validity of the theory, the performance of new products has been evaluated. Table I and II show the specification of the products and the employed IGBTs, respectively. Figures 4 and 5 show the appearance of the new product and the power units of the new and conventional products, respectively.

Table I shows that the dc voltage fed from the solar-cells varies in wide range (i.e., 80 to 350 [V_{AVE}]) due to the Maximum Power Tracking. Although the rated utility voltage is 220 [V_{RMS}], it can reach much higher value in practice and a case of 280 [V_{RMS}] has been

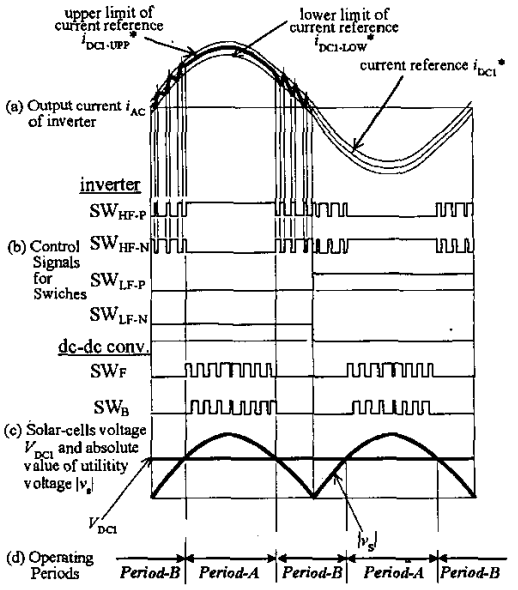

Fig. 3. Operating principle of Inverter and DC-DC converter.
Only the inverter (in Period-A) or the dc-dc converter (in Period-B) is operated with high-frequency PWM to waveshape the utility current and thus, losses caused by PWM is reduced significantly.

considered in the design. The IGBTs (with the ratings of 600 [V] and 60 [A] and package of TO3-P) are employed in the all switches but those in the high-frequency half-bridge and dc-dc converter are fast-type while those in the low-frequency half-bridge are slow-type, as shown in Table II. The forward voltage drops (or collector-emitter saturation voltages) of the fast- and slow-type IGBTS are 1.55 [V] and 1.25 [V] (@ I_C=60[A]), respectively.

As seen in Fig. 5, the power unit of the new product is compact and the size is approximately 2/3 of that of the conventional one. This size-reduction is achieved due to less size of the heat sink (i.e. less power losses) and less of one electrolytic capacitor.

Fig.6 and 7 show operating waveforms of the new product while Table III shows circuit condition and measured data. The waveforms shown in Fig. 6 and 7 have been obtained under the condition shown in Table III. The waveform of the intermediate dc voltage v_{DC2} (top trace in Fig. 6) shows that the voltage equals the absolute value of the utility voltage v_S (220 [V_{RMS}] and the maximum value is 311 [V] for this case) in Period-A, as discussed in the theory. The middle and bottom traces in Fig.6 show the waveforms of the current i_{SW-F} and voltage v_{SW-F} of the boost switch SW_F in the Period-A. It can be seen from these switching waveforms that the IGBT offers very fast switching in turn-on and turn-off. The spike current occurring at the turn-on instant of the switch SW_F is due to reverse recovery of the reverse conduction diode D_B.

On the other hand, the dc voltage v_{DC2} is higher than the

Table I. Specification of Product

Items	Data
Rated Output Power	4.5 [kW]
DC Voltage Fed from Solar-Cells	80 – 350 [V_{AVE}]
Rated Utility Voltage	220 [V_{RMS}] (1-phase 3-wire)
Utility Frequency	50 or 60 [Hz]
Cooling	Natural Air Cooling
Size	550 x 300 x 124 [mm] (20 [litters])
Weight	20 [kg]

Table II Specifications of IGBTs

Items	Specifications GT60J321 (Fast Type)	GT60j322 (Slow Type)
Coll.-Emit. Voltage (V_{CES})	600 [V]	
Collector Current (I_C)	60 [A] @ DC, 120 [A] @ 1[ms] pulse	
Collector-Emitter Saturation Voltage ($V_{CE(sat)}$)	1.2[V] @ I_C=10[A] 1.55[V]@I_C=60[A]	0.9[V] @ I_C=10[A] 1.25[V]@I_C=60[A]
Turn-ON time (t_{ON})	0.40[μs]	0.3[μs]
Turn-OFF time (t_{OFF})	0.65[μs]	1.40[μs]
Emit.-Coll. Voltage (V_F)	1.5[V] @ I_F=60[A]	1.2[V] @ I_F=60[A]
Reverse-recovery time (t_{rr})	0.1[μs] @ I_F=60[A]	0.6[μs] @ I_F=60[A]

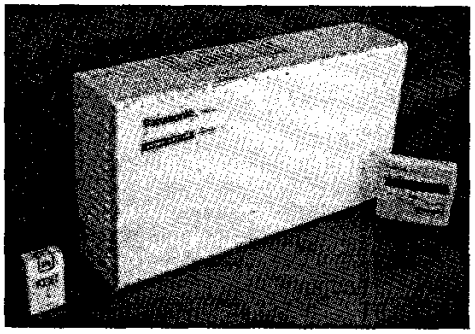

Fig. 4. Appearance of Product.

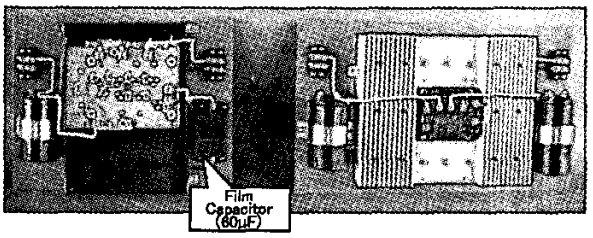

Fig. 5. Power Units in New (left) and Conventional (right) Products.

The size in the new product is 2/3 of the conventional one, and the left-hand-side electrolytic capacitor in conventional product has been replaced by a film capacitor in the new product.

absolute value of the utility voltage v_S in the remaining period (i.e., Period-B). In this period, the boost dc-dc converter cannot operate and it interrupts the operation. Thus, the dc-capacitor C_1 is connected to the dc-capacitor C_2 though the dc-inductor L_1 and reverse conducting diode D_B. As a result, the intermediate dc voltage v_{DC2} produces an oscillation caused by L_1 and C_2 as shown in Fig. 6, where the effect of C_1 on the oscillation is negligible since the capacitance is large enough compared with C_2. This oscillation, however, is not so significant and no damage is produced in this system. In this period, the inverter operates with high frequency switching to perform the Bang-Bang control for the ac current i_{AC}. However, an alternative topology to avoid the oscillation is introduced later.

Fig. 7 shows the waveform of the utility current i_S. From this waveform, we can recognize that the waveshaping by the boost dc-dc converter and the inverter with the Bang-Bang control has been operated ideally. The

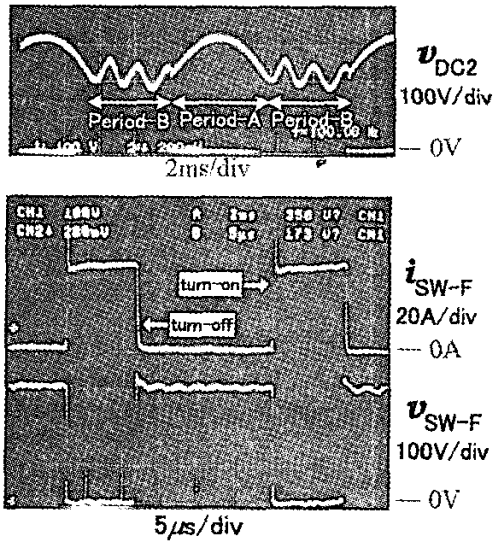

Fig. 6. Operating Waveforms.

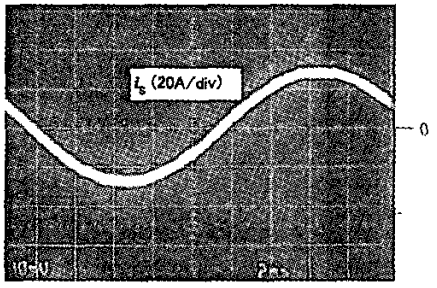

Fig. 7. Operating Waveform of Utility Current i_S.

Table III
Circuit Condition and Measured Data for Operating Waveforms in Fig. 4 and 5.

Items	Data
DC-Inductors (L_1 and L_2)	1.0 mH
DC-Capacitor (C_1)	2,000 μF
DC-Capacitor (C_2)	60 μF
Output Power ($P_{O\text{-}RAT}$)	4.5 kW
DC Voltage Fed from Solar Cell (V_{DC1})	208 V_{AVE}
Utility Voltage (V_S)	220 V_{RMS}
Utility Frequency (f_S)	50 Hz
Efficiency (η)	95.2 %
Total Harmonic Distortion of Utility Current i_S ($THD\text{-}i_S$)	1.6 %

Total-Harmonic-Distortion *THD-i*$_S$ of the current is only 1.6 [%].

Fig. 8 shows efficiency curves for the power P_S fed to the utility where the dissipated power of 30 [W] in the controller has been taken into account. The efficiency has marked very high value and is more than 95.5 [%] and 95 [%] at the medium and full load condition, respectively, under the condition of V_S = 240 [V_{RMS}]. Thus, the effect of the novel current modulation scheme (i.e., alternation of high-frequency switching operation between the boost converter in Period-A and the inverter in Period-B) to reduce the switching losses has been confirmed. Table IV shows a loss analysis for the condition of P_S = 4.5 [kW] and V_S = 208 [V_{RMS}] where the efficiency is 94.5 [%] and the total loss is 261 [W]. It can be known from the table that the power dissipation of the power devices is low and it results in the high efficiency. The efficiency in the maximum power condition increases by 0.67 [%] if the power dissipation of the controller (30 [W]) is omitted.

By the way, the oscillation caused by L_1 and C_2 (refer to the top trace in Fig. 6) may cause acoustic noise produced by L_1. By employing the additional diode D_S shown in Fig. 1, the oscillation can be eliminated as shown in Fig. 9. The dc capacitor C_2 is connected to C_1 through the diode D_S in the modified topology, and thus the oscillation does not occur. The performance, including the current waveform quality and the efficiency, of the system with the modified topology with D_S are almost the same to those of the original topology without D_S.

V. CONCLUSION

A novel utility-interactive inverter for photovoltaic system has been proposed and its power circuit topology and current control scheme have been introduced. Further, the validity of the theory has been confirmed through experimental results obtained from a real product with output power of 4.5 [kW]

By means of the proposed techniques, the utility-interactive inverter has been improved in efficiency, size, weight and cost. The efficiency of the product under the maximum and medium output power has marlked 95 and 95.5 [%], respectively, both for the utility voltage of 240 [V_{RMS}]. The size of the power units decreased to 2/3 of that of the conventional one. Further, the cost has been decreased due to the size reduction and the utilization of cheap IGBTs with low switching performance in the inverter. Additionally, a modified topology to avoid the low-frequency oscillation between the dc inductor and the dc capacitor has been introduced and its effect has been confirmed practically.

The technique applied on the new inverter and based on controlling instantaneous dc inductor current (i.e., instantaneous dc inductor stored energy) is applicable in managing low-frequency ripple energy in single-phase AC to DC and three-phase AC to avoid balky energy storage components. Detail study in the application remains.

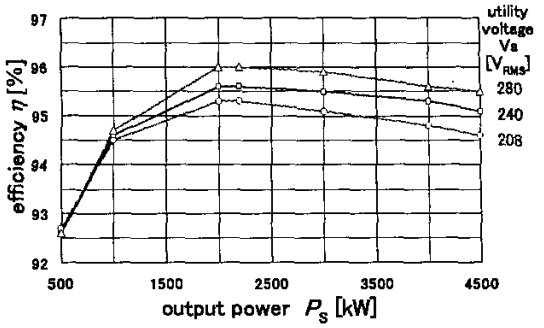

Fig. 8. Measured Efficiency.

A very high Efficiency has been obtained especially in medium load condition.

Table IV
Loss Analysis for Condition of P_S = 4.5 [kW] and V_S = 208[V_{RMS}]

Items	Losses [W]
Power Devices in DC-DC Converter (SW_B & SW_F)	72
DC-Inductor (L_1)	52
DC-Capacitor (Film Capacitor: C_2)	5
Power Devices in Inverter	53
DC-Capacitor (Electrolytic Capacitor: C_1)	5
AC-Inductor (L_2)	28
Control Circuitry	30
Others	16
Total	261

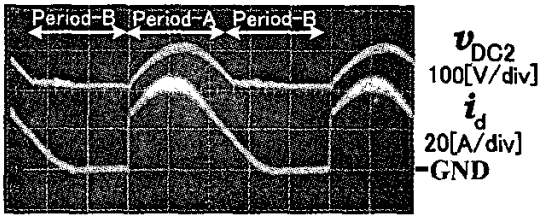

Fig. 9. Operating Wafeforms of Modified Toplogy with Diode D_S.

The oscillation in Period-B has been disappeared. The current i_d of the dc-inductor L_1 flows even in the beginning half of the Period-B to discharge the stored energy.

REFERENCES

[1] S. Sumiyoshi, H. Terai, T. Kitaizumi, T. Okude, H. Omori, Y. Nishida and M. Nakaoka, "Practical Evaluation of Single-Ended Resonant Utility Interactive Inverter," Proc. of IPEC-Tokyo, Vol. 3, pp. 1680-1685 (March 2000 in Tokyo)

[2] Y. Nishdia, S. Motegi and A. Maeda, "A Single-Phase Buck-Boost AC-to-DC Converter with High-Quality Input and Output Waveforms," Proc. of the IEEE ISIE, Vol. 2, pp. 433-438 (July 1995 in Athens)